Magnetotransport in carbon foils fabricated from exfoliated graphite

van Schaijk, R.T.F.; de Visser, A.; Kulbachinskii, V.A.; Kytin, V.G.; Ionov, S.G.

Link to publication

Magnetotransport in carbon foils fabricated from exfoliated graphite

R. T. F. van Schaijk[*] and A. de Visser

Van der Waals-Zeeman Institute, University of Amsterdam, Valckenierstraat 65, 1018 XE Amsterdam, The Netherlands

S. G. Ionov, V. A. Kulbachinskii, and V. G. Kytin

Low Temperature Physics Department, Moscow State University, 119899 Moscow, Russia

(Received 29 April 1997; revised manuscript received 3 October 1997)

The magnetotransport properties of a series of low-density carbon foils, fabricated from exfoliated graphite, prepared with different densities and subjected to different heat treatments, have been investigated. The Hall resistance and the magnetoresistance were measured at low temperatures ($T > 0.4$ K) in magnetic fields up to $B = 8$ T. The transport properties showed the main features of weak localization, i.e., a logarithmic temperature variation of the resistivity and a negative magnetoresistance for $B < 0.5$ T at low temperatures. The negative contribution to the magnetoresistance has been analyzed within the model of Wittmann and Schmid for weak localization beyond the diffusion limit. The analysis yields the phase relaxation time τ_φ of the carrier wave function. The structural analysis of the carbon foils shows that the weak localization must be attributed to the disorder in the stacking sequence of the graphene planes. [S0163-1829(98)08515-4]

I. INTRODUCTION

Because of their strongly layered structure, graphite and graphite-based materials, such as graphite intercalation compounds, offer interesting perspectives to investigate physical phenomena related to reduced dimensionality.[1–4] The quasi-two-dimensional behavior of the charge carriers is reflected in a large ratio of the electrical conductivity along the a and the c axis, σ_a / σ_c, which attains a value of $\sim 10^4$ in single-crystalline graphite.[2] Upon separating the graphene sheets by acceptor-type intercalants, the conductivity anisotropy can be enhanced significantly to values as large as $\sim 10^6$ in AsF$_5$ stage-1 intercalated graphite.[5] Indeed, graphite intercalation compounds can be used to study dimensionality crossover phenomena, such as the warping of the cylindrical Fermi surface as disclosed by Shubnikov–de Haas oscillations in the magnetotransport data.[6] Another arresting physical phenomenon that has been reported for graphite-based materials is two-dimensional weak electron localization.[2,3,7]

Weak localization[8] originates from the quantum-mechanical interference between elastically scattered carrier waves. Inelastic-scattering processes destroy the phase coherence between the carrier waves and therefore weak localization predominantly takes place at low temperatures. An applied magnetic field also destroys the phase coherence between the carrier waves. The two main experimentally accessible features of weak electron localization are a logarithmic temperature dependence of the electrical resistivity and a negative magnetoresistance in low magnetic fields. Weak electron localization leads to quantum corrections to the classical Boltzmann expression for the electrical conductance. These quantum corrections are larger when the dimensionality of the system is lower and become more and more important when the amount of disorder increases. A most relevant study in this respect was performed by Bayot *et al.*,[7] who investigated the magnetotransport properties of partially graphitic carbons. The observed negative magnetoresistance and the low-temperature behavior of the resistivity of a series of pyrocarbon samples,[7] subjected to different heat treatments, could be well accounted for by the theory of two-dimensional (2D) weak electron localization.

In this paper, we report the results of a low-temperature study of the magnetotransport properties, i.e., the magnetoresistance and Hall effect of carbon foils fabricated from exfoliated graphite. Pregraphitic materials, like exfoliated graphite, exhibit a random stacking of the graphene layers (turbostratic structure), in contrast to graphite crystals in which the stacking is regular (predominantly $ABAB\dots$) (see Ref. 2). The amount of disorder in the stacking sequence is expected to play an important role in the weak-localization process. The experiments were carried out on samples subjected to different heat treatments and with different structural parameters. The magnetotransport data were analyzed with help of the theory of anomalous magnetoconductance beyond the diffusion limit, as formulated by Wittmann and Schmid.[9]

II. EXPERIMENTAL

A. Sample preparation

As starting material for the preparation of the exfoliated graphite foils we used highly oriented pyrolitic graphite annealed at a temperature $T > 3300$ K. The angle of misorientation with respect to the c axis was less than 1°. First, a stage-1 H$_2$SO$_4$ graphite intercalation compound was prepared by the liquid phase method with K$_2$Cr$_2$O$_7$ as the oxidizer.[10] The intercalation process of graphite with H$_2$SO$_4$ was controlled *in situ* by x-ray-diffraction and resistivity measurements. By intercalation, the intergraphite layer spacing increased from 3.35 until 7.98 Å. After hydrolization and drying the sample was exfoliated at 900 °C. The exfoliation process leads to a rapid blowup of the interlayer spacing. The intercalate evaporates and the volume of the sample increases a factor of 200–300. Foils with different densities were fabricated by rolling the exfoliated graphite. By rolling, the layers collapse in a way that the stacking becomes disor-

TABLE I. Structural parameters of exfoliated graphite foils $N4$ and $N6$ prepared with different densities D and annealed at different temperatures. HTT is the heat-treatment temperature, d_0 is the interlayer spacing, p_t is the turbostratic probability parameter, defined in the text, and α is the mosaic spread. The parameters d_0 and α have been determined by x-ray experiments.

Sample	D (g/cm^3)	HTT (°C)	d_0 (Å)	p_t	α
$N4$	0.70		3.365	0.28	7.7°
	0.70	2100	3.364	0.26	
	0.70	2400	3.361	0.20	
	0.70	2800	3.361	0.20	
$N6$	0.85		3.367	0.30	6.6°
	0.85	2100	3.365	0.28	
	0.85	2400	3.362	0.21	
	0.85	2800	3.360	0.19	7.0°

dered. The final thickness of the foils amounted to 0.5 mm. Part of the foils were heat treated at temperatures [heat treatment temperature (HTT)] of 2100, 2400, and 2800 °C. The different densities allow for a study of the effect of intergrain scattering. For a complete description of the sample fabrication process we refer to Ref. 11.

B. Measuring techniques

For the magnetotransport experiments specimens with typical dimensions of $3 \times 10 \times 0.5$ mm^3 were cut from the foils. The magnetotransport measurements were carried out using a conventional four-point low-frequency ac technique with a typical excitation current of 300 μA. The current was directed along the longest direction of the sample. Voltage and current leads were connected to the samples using silver paint. The samples were attached to the cold-plate of a ^{3}He system, employing a charcoal adsorption pump to reach the base temperature (300 mK). As thermometer served a RuO$_2$ thick-film chip resistor. Magnetic fields up to 8 T, provided by a superconducting solenoid, were directed perpendicular to the surface of the foils (predominantly $B\|c$). The magnetoresistance of the thermometer is small and could be neglected.

III. RESULTS

A. Structural parameters

Two series of rolled samples were studied with densities of 0.70 and 0.85 g/cm^2, labeled $N4$ and $N6$, respectively. The structural parameters of the investigated exfoliated graphite foils are reported in Table I. The carbon foils consist of grains with sizes of the order of several hundred Angstrom. As the grains are not perfectly aligned with the c axis perpendicular to the surface of the foils, the foils show mosaicity. The mosaic spread (α) due to angular variation of the c axis with respect to the surface of the foils has been determined for samples $N4$ and $N6$ by x-ray diffraction. Values for α amount to 7° (see Table I). No significant variation of α upon rolling to the different densities has been observed.

For each series of foils heat treatments were given at temperatures of 2100, 2400, and 2800 °C. Annealing decreases the amount of disorder in the stacking sequence.[7] The influ-
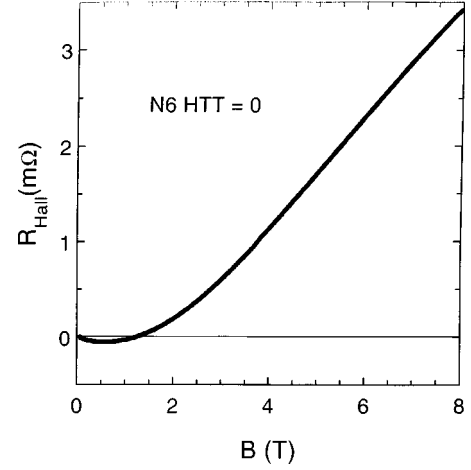

FIG. 1. Hall resistance as function of the magnetic field for sample $N6$ (HTT=0) at $T=4.2$ K. Because the conduction at low temperatures is by electrons as well as holes, the Hall resistance is nonlinear and changes sign.

ence of stacking faults can be investigated as function of the heat treatment temperature. The interlayer spacing (d_0), determined by x-ray diffraction, shows a weak dependence on the heat-treatment temperature (see Table I). For single-crystalline graphite $d_0=3.354$ Å, while for a fully turbostratic structure $d_0=3.440$ Å (Ref. 7). The measured values are close to that of graphite, which shows that only a fraction of the layers are turbostratic. Apparently, preparation of the exfoliated graphite foils as described in the previous section, has only a small effect on the periodicity along the c axis. The probability of finding two neighboring graphene layers of a partially turbostratic sample in a randomly stacked configuration is given by[12]

$$p_t = \sqrt{11.63 d_0 - 39}, \qquad (1)$$

where d_0 is given in Ångstrom. The values for p_t are listed in Table I. For $p_t=0$, the sample is a perfect three-dimensional single crystal, while for $p_t=1$ the crystal is fully turbostratic. We did not observe a clear transition from
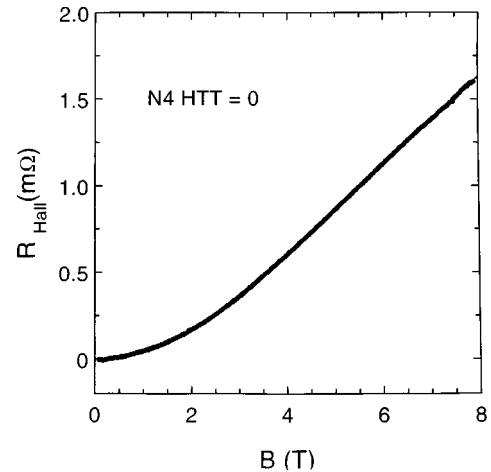

FIG. 2. Hall resistance as function of the magnetic field for sample $N4$ (HTT=0) at $T=4.2$ K.
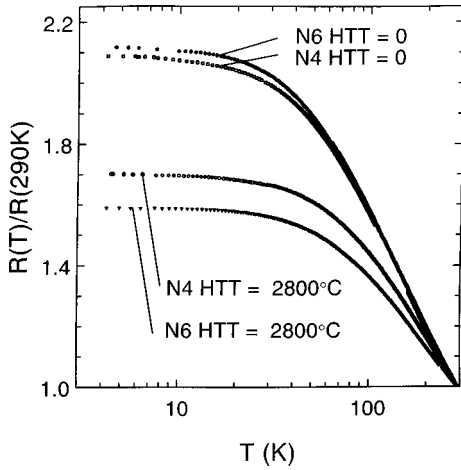
FIG. 3. Resistance, normalized at $T = 290$ K, versus $\ln T$ for samples $N4$ and $N6$ with HTT=0 and 2800 °C as indicated.

turbostratic to graphitic in this range of HTT's, as was, for instance, reported for pyrolitic graphite in the range 2100–2400 °C (Ref. 7).

In Sec. IV we will analyze the magnetotransport data in terms of the theory of weak localization in two dimensions. For this analysis it is important to know the amount of graphene layers in the foils in order to transform the 3D carrier density, derived by the Hall-effect measurements, into a 2D carrier density. The amount of layers A is calculated by

$$A = \frac{\lambda d}{d_0}, \qquad (2)$$

where d is the thickness of the sample and $\lambda = D/2.265$. D is the density in g/cm^3 and λ is a factor which describes the inhomogeneity of the sample. This inhomogeneity is caused by the free space between the layers, when the sample is not a closed stack. The numerical value of 2.265 g/cm^3 in the expression for λ is the density of single-crystalline graphite.[2]

B. Hall effect

The Hall effect has been measured for samples $N4$ and $N6$ with no heat treatment (HTT=0) and a HTT of 2800 °C.

TABLE II. Resistivity values at $T = 4.2$ K and $T = 300$ K for exfoliated graphite foils $N4$ and $N6$ with HTT=0 and HTT=2800 °C

Sample	HTT (°C)	$\rho_{4.2\,K}$ (mΩ cm)	$\rho_{290\,K}$ (mΩ cm)
$N4$		1.6	0.95
	2800	2.3	1.1
$N6$		1.9	1.2
	2800	1.8	0.87

Data have been taken at 0.4 and 4.2 K in fields up to 8 T. The Hall resistance (R_{Hall}) was found to be independent of temperature in the range 0.4–4.2 K. An exemplary curve, measured for sample $N6$ (HTT=0) at $T = 4.2$ K, is shown in Fig. 1. The Hall resistance shows strong deviations from the standard linear behavior, and at low magnetic fields R_{Hall} changes sign. Similar nonlinear curves were obtained for sample $N4$ (HTT=0), but R_{Hall} did not change sign (see Fig. 2). We infer that, at low temperatures, the current in our exfoliated graphite foils is carried by electrons as well as holes.[13]

C. Resistivity and magnetoresistance

In Fig. 3, the temperature dependence of the normalized resistance between 4.2 and 290 K is shown for samples $N4$ and $N6$ with HTT=0 and 2800 °C. For both sets of samples, the resistance increases with decreasing temperature. In Fig. 4, the low-temperature ($T < 10$ K) normalized resistance is presented. Only for $T < 2$ K, the resistance shows a logarithmic temperature dependence. In Table II, we have listed the resistivities $\rho(4.2$ K) and $\rho(300$ K) for the various samples.

The magnetoresistance up to 8 T at $T = 4.2$ K of sample $N6$, heat treated at 2800 °C, is shown in Fig. 5. At small fields ($B < 1$ T), the magnetoresistance varies quadratically with field and is attributed to the normal Lorentz term. At higher fields the magnetoresistance varies approximately lin-
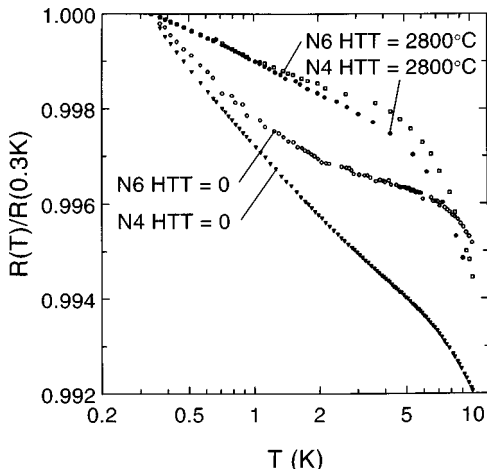

FIG. 4. Resistance, normalized at $T = 0.3$ K, versus $\ln T$ for samples $N4$ and $N6$ with HTT=0 and 2800 °C as indicated. For $T < 2$ K a logarithmic temperature variation is observed.
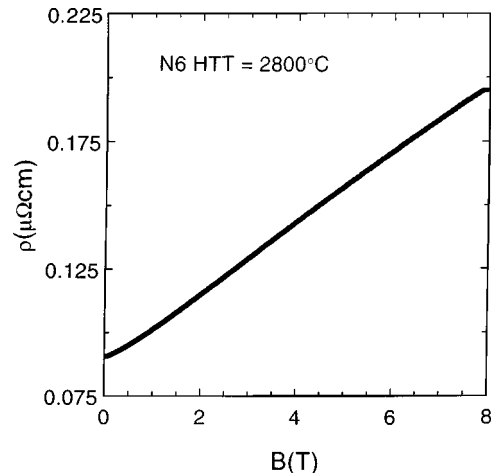

FIG. 5. Resistivity as function of the magnetic field for sample $N6$ with HTT=2800 °C at $T = 4.2$ K. At small magnetic fields there is a quadratic dependence on field, which becomes linear at fields above 1 T.
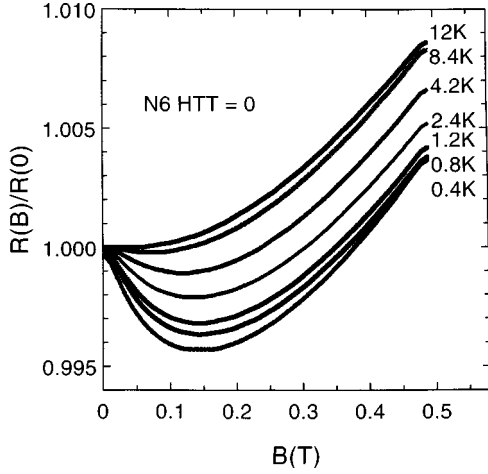
FIG. 6. Magnetoresistance, normalized at $B=0$, versus magnetic field for sample $N6$ (HTT=0) at temperatures between 0.4 and 12 K as indicated.

early with field. In Figs. 6–9 the magnetoresistance data for $B<0.5$ T of samples $N6$ and $N4$ with HTT= 0 and 2800 °C, are presented. At low temperatures and low magnetic fields the magnetoresistance is negative. Above a certain temperature, only the positive component to the magnetoresistance is present. The difference between the magnetoresistance of samples $N4$ and $N6$ is small, especially for the heat-treated samples.

IV. ANALYSIS

A. Hall effect

The Hall resistance data, presented in Figs. 1 and 2, show strong deviations from the standard linear behavior. This strongly suggests that the charge carriers in exfoliated graphite are electrons *and* holes. We fitted $R_{\text{Hall}}(B)$ to the well-known formula derived for a two-band system. Under the conditions that the electronic system has spherical constant energy surfaces and the elastic relaxation time is constant, one can show[14]
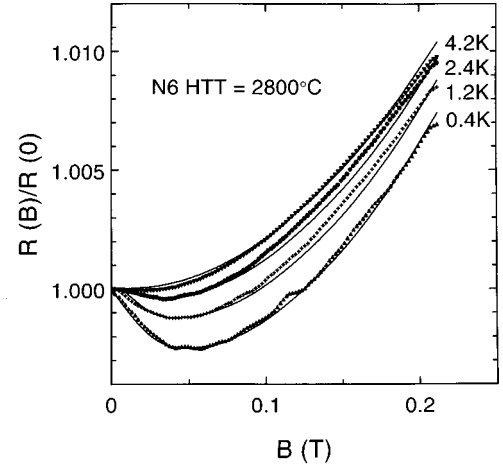

FIG. 7. Magnetoresistance, normalized at $B=0$, versus magnetic field for sample $N4$ (HTT=0) at temperatures between 0.4 and 12 K as indicated. The various symbols represent the data points. The solid lines represent the best fit to Eq. (8).

FIG. 8. Magnetoresistance, normalized at $B=0$, versus magnetic field for sample $N6$ (HTT=2800 °C) at temperatures between 0.4 and 4.2 K as indicated. The various symbols represent the data points. The solid lines represent the best fit to Eq. (8).

$$R_{\text{Hall}} = \frac{(p-nm^2)+m^2m_h^2B^2(p-n)}{(p+nm)^2+m^2m_h^2B^2(p-n)^2}\left(\frac{B}{e}\right).\quad (3)$$

Here $m=\mu_e/\mu_h$, μ_e and μ_h are the mobility of electrons and holes, respectively, n and p are the concentrations of electrons and holes, respectively, and B is the magnetic field. Values for m, μ_h, n, and p are derived from the Hall measurements by least-squares fits to Eq. (3). The derived fit parameters yield the total 3D carrier densities and mobilities, and are listed in Table III.

B. Resistivity and magnetoresistance

1. Theory

Under the same conditions as the Hall resistance, the Lorentz term in the transverse magnetoresistance is given by[14]

$$\frac{-\Delta\sigma}{\sigma_0} = \frac{\Delta\rho}{\rho_0} = \frac{npm(1+m)^2\mu_h^2}{(nm+p)^2}B^2.\quad (4)$$

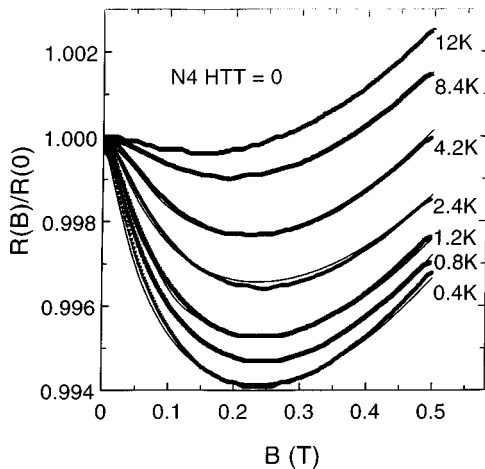FIG. 9. Magnetoresistance, normalized at $B=0$, versus magnetic field for sample $N4$ (HTT=2800 °C) at temperatures between 0.4 and 4.2 K as indicated. The various symbols represent the data points. The solid lines represent the best fit to Eq. (8).
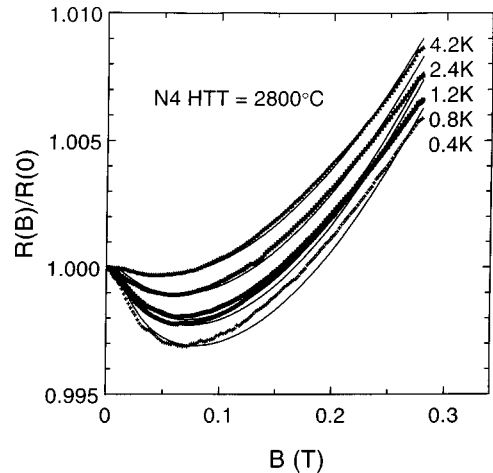
TABLE III. Carrier densities of exfoliated graphite samples $N4$ and $N6$ as determined from fits of the Hall resistance to Eq (3). HTT is the heat-treatment temperature, n is the electron density, p is the hole density, n_{total} is the two-dimensional density of electrons and holes, and λ is an inhomogeneity factor defined in the text.

Sample	HTT	n (cm^{-3})	p (cm^{-3})	n_{total} (cm^{-2})	λ
$N4$		2.8×10^{18}	5.1×10^{18}	1.6×10^{13}	0.31
	2800 °C	7.0×10^{17}	1.8×10^{18}	4.9×10^{12}	0.30
$N6$		6.8×10^{17}	1.2×10^{18}		0.37
	2800 °C	2.3×10^{18}	3.2×10^{18}	1.3×10^{13}	0.37

Here σ_0 and ρ_0 are the conductivity and resistivity, respectively, at $B=0$. This quadratic dependence is only valid for small values of the magnetic field ($B<1$ T). For $B>1$ T the dependence becomes quasilinear (see Fig. 5). At low fields and low temperatures ($T\leq4.2$ K), in addition to the B^2 term, a pronounced negative magnetoresistance component is observed.

The logarithmic increase of the resistance with decreasing temperature (see Fig. 4) and the negative magnetoresistance (see Figs. 6–8) are attributed to quantum corrections to the conductivity for the two-dimensional case.[15] An analysis within such a framework yields the possibility to determine characteristic parameters of the electron wave function, like the wave function phase relaxation time τ_φ. The phase relaxation time depends on the strength of the electron-electron and electron-phonon interactions. The temperature dependence of the conductivity of two-dimensional disordered systems in zero magnetic field due to quantum corrections is given within the theory of Al'tshuler and Aranov[15] by

$$\sigma(T_2)-\sigma(T_1)\propto\frac{e^2}{2\pi^2\hbar}\ln\left(\frac{T_2}{T_1}\right). \qquad (5)$$

The logarithmic temperature variation of σ due to weak localization allows one to determine $\tau_\varphi(T)$. However, in addition to the weak-localization effect, a similar logarithmic contribution is expected if the mutual Coulomb interaction of the electrons is taken into account.[15,16] The effect of the electron-electron interaction and the weak localization can be distinguished by magnetotransport experiments in a perpendicular magnetic field. The weak-localization effect is strongly suppressed by a magnetic field, which results in a negative magnetoresistance, while the electron-electron effect is hardly influenced. Therefore, data of the resistance in constant magnetic field could, in principle, be used to determine the effects of weak localization and electron-electron interactions. However, in our case the dominating background resistance and its field dependence cannot be estimated accurately, which hampers an adequate analysis using Eq. (5). Another route to determine $\tau_\varphi(T)$ is by directly measuring the negative magnetoresistance. Detailed theories for weak electron localization have been worked out by Al'tshuler and Aranov,[15] Hikami, Larkin, and Nagaoka,[17] and Wittmann and Schmid.[9] In the theories of Al'tshuler and

Aranov and Hikami, Larkin, and Nagaoka it is assumed that the diffusion limit is valid. The diffusion limit is expressed by the following relations:

$$\gamma=\frac{\tau_0}{\tau_\varphi}\ll1 \quad \text{and} \quad b=\left(\frac{l_0^{\text{eff}}}{l_B}\right)^2\ll1. \qquad (6)$$

Here τ_0 is the elastic relaxation time and τ_φ is the wavefunction phase relaxation time, defined by inelastic-scattering events. The effective mean free path l_0^{eff} is described by $l_0^{\text{eff}}=l/(1+\gamma)=\sqrt{(2E_f/m^*)}\tau_0/(1+\gamma)$, where $E_f=\pi\hbar^2 n/m^*$. Here $m^*(=0.06m_e)$ is the effective mass,[2] n is the 2D carrier density, and $l_B=\sqrt{(\hbar/2eB)}$ is the magnetic length.

We first fitted the negative magnetoresistance (Figs. 6–9) to the theory of Al'tshuler and Aranov. However, we could not obtain satisfactory fit results in the relevant field range, which suggested that the diffusion limit is not valid. Indeed, for instance, for sample $N4$ (HTT=0) we obtain $b=10B$, thus in our exfoliated graphite foils the limit $b\ll1$ is only valid for very small magnetic fields. We then analyzed the data within the model of Wittmann and Schmid,[9] which is also valid beyond the diffusion limit. According to Wittmann and Schmid, the quantum correction to the conductivity in a magnetic field is given by

$$\Delta\sigma(B)=\frac{-e^2}{2\pi^2\hbar}\frac{b}{(1+\gamma)^2}\sum_{n=0}^{\infty}\frac{\Psi_n^3(b)}{1+\gamma-\Psi_n(b)}, \qquad (7)$$

where

$$b=\frac{2el^2B}{(1+\gamma)^2\hbar}$$

and Ψ_n are the Laguerre polynomials:

$$\Psi_n(b)=\int_0^{\infty}e^{-(\zeta+b\zeta^2/4)}L_n(b\zeta^2/2)d\zeta$$

with

$$L_n(y)=\sum_{m=0}^{n}\frac{1}{m!}\binom{n}{m}(-y)^m.$$

2. Analysis

For the analysis of the magnetotransport data of the exfoliated graphite foils, we make the assumption that the measured magnetoresistance can be expressed as the sum of two terms:

$$\left(\frac{\Delta R(B)}{R(0)}\right)_{\text{exp}}=-p_t^2\frac{\Delta\sigma(B)}{\sigma(0)}+\left(\frac{\Delta R(B)}{R(0)}\right)_{\text{Lorentz}}. \qquad (8)$$

The contribution from the weak localization, $\Delta\sigma(B)$, is given by Eq. (7) and $(\Delta R(B)/R(0))_{\text{Lorentz}}$ is given by Eq. (4). Equation (8) is only valid when the magnetic field is directed perpendicular to the 2D structure ($B\|c$), which is formed in exfoliated graphite by the graphene layers. The relatively small mosaicity of the grains ($\alpha\approx7°$) could be neglected.

The random stacking probability parameter p_t plays an important role in the quantitative analysis of the weak-

TABLE IV. Relaxation times and mobilities of exfoliated graphite foils $N4$ and $N6$ at temperatures T as indicated. The relaxation times are determined by fitting the magnetoresistance data to Eq. (8). HTT is the heat-treatment temperature, μ is the mobility, τ_0 is the elastic relaxation time, and τ_ϕ is the phase relaxation time.

| Sample	HTT	T (K)	μ (m^2/Vs)	τ_0 (s)	τ_ϕ (s)
$N4$		0.4	0.087	2.95×10^{-14}	8.6×10^{-13}
		0.8	0.085	2.89×10^{-14}	7.0×10^{-13}
		1.2	0.085	2.88×10^{-14}	6.0×10^{-13}
		2.4	0.084	2.87×10^{-14}	4.5×10^{-13}
		4.2	0.084	2.85×10^{-14}	3.4×10^{-13}
$N4$	2800 °C	0.4	0.29	9.9×10^{-14}	1.7×10^{-12}
		0.8	0.29	9.8×10^{-14}	1.2×10^{-12}
		1.2	0.29	9.8×10^{-14}	1.1×10^{-12}
		2.4	0.28	9.7×10^{-14}	6.9×10^{-13}
		4.2	0.28	9.6×10^{-14}	4.2×10^{-13}
$N6$	2800 °C	0.4	0.21	7.1×10^{-14}	6.5×10^{-12}
		1.2	0.20	6.9×10^{-14}	1.1×10^{-12}
		2.4	0.20	6.9×10^{-14}	4.8×10^{-13}
		4.2	0.20	6.8×10^{-14}	1.8×10^{-12}

FIG. 10. Temperature dependence of the wave-function phase relaxation time τ_φ as determined for sample $N4$ (HTT=0) using Eq. (8) (data listed in Table IV). The data points are the result from the fits and the line is a fit according to Eq. (9).

localization process. For pure homogeneous graphite structures a negative contribution to the magnetoresistance is absent, while in inhomogeneous graphite structures a negative $\Delta\sigma(B)$ occurs quite general.[2] The most common inhomogeneity or structural defect in the graphite lattice is the breaking of the $ABAB$ periodicity along the c axis, i.e., turbostratic layers are formed (e.g., $ABCAB\ldots$). The probability that a layer is turbostratic is given by p_t.[2] The charge carriers are scattered elastically at these lattice defects. Following Bayot et al.[7] we presume that the stacking disorder is the main cause for the weak localization. Since only turbostratic layers are responsible for the negative magnetoresistance, $\Delta\sigma(B)$ is multiplied by p_t.[2] Values for p_t are listed in Table I.

In order to fit the magnetoresistance data (Figs. 6–9) to Eq. (8), we made use of the following procedure. First, the 3D electron (n_e) and hole (n_h) densities, obtained by fitting the Hall data (Figs. 1 and 2), were transformed to average 2D densities with help of Eq. (2). Next the values for the electron (μ_e) and hole (μ_h) mobilities, obtained by fitting the Hall data, were averaged and transformed into an effective elastic-scattering relaxation time τ_0. Finally, the magnetoresistance data were fitted to Eq. (8). Since for all samples R_{Hall} was determined at $T=4.2$ K, τ_0 was used as a known variable at this temperature. At lower temperatures τ_0 was used as a fit parameter. The temperature variation $\tau_0(T)$ is small, which is consistent with R_{Hall} being temperature independent in this temperature range. Fitting was done using the least-squares method. An advantage of using the theory of weak localization of Wittmann and Schmid in Eq. (8), is that once reliable values for τ_0 are known, the only important fit parameter is τ_φ. In Figs. 7–9, we compare the experimental magnetoresistance for samples $N4$ and $N6$ with $\Delta R(B)/R(0)$, calculated with the help of Eq. (8) (solid lines), using the best-fit parameters τ_0 and τ_φ. The agreement is good. The resulting values for τ_0 and τ_φ are listed in Table IV.
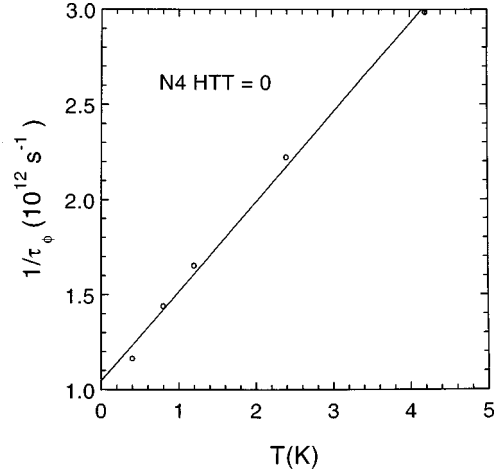
In general, the temperature dependence of the phase relaxation time $\tau_\varphi(T)$ is given by a power law with exponent q:[15]

$$\tau_\varphi = cT^{-q}. \tag{9}$$

In the case of dominant electron-electron scattering in weakly disordered metals, it was found that $q=d/2$ (Ref. 15), where d is the dimensionality. For the 2D case, $q=1$. In Fig. 10 we show the typical variation of τ_φ with temperature as obtained for sample $N4$ (HTT=0). Clearly, $\tau_\varphi(T)$ does not obey the predicted power law [Eq. (9)]. If we suppose that $(\tau_\varphi)^{-1}=(\tau^*)^{-1}+(\tau_{\text{in}})^{-1}$, where τ_{in} is a temperature-independent inelastic-scattering time in the investigated temperature range, then τ^* obeys a power law with exponent $q\approx1$.

V. DISCUSSION

The aforementioned theories for weak localization are all derived for one type of carrier. In the case of the exfoliated graphite foils, electrons as well as holes carry the current. The derived parameters should thus be considered as an effective weighted average over the two types of carriers. Rainer and Bergmann[18] showed that the theory of weak localization is universal in the sense that multiband effects do not effect the weak localization. In this respect, we may consider the magnetotransport properties of our graphite structures as arising from a multiband system.

After annealing at high temperatures, the negative contribution to the magnetoresistance becomes weaker (compare Fig. 6 with Fig. 8 and Fig. 7 with Fig. 9). This effect is due to a decrease in disorder by annealing. As p_t decreases significantly by annealing (see Table I), the weak localization can be connected to the amount of turbostratic layers p_t. The negative magnetoresistance contribution does not change significantly with the density (at least for the density range we investigated), which indicates that intergrain scattering processes do not play an essential role. The phase relaxation time is of the same order for samples $N4$ and $N6$. Also the

method of preparation of the foils (rolling or pressing[11]) has a minor influence.

Like Bayot *et al.*,[7] we conclude that a random stacking of graphene layers (turbostratic structure) is the main cause for the occurrence of the weak-localization phenomenon. As p_t is relatively small for our exfoliated graphite samples, the quantum correction to the conductivity is small when compared to the effects observed by Bayot *et al.*[7] in partially graphitic carbon. Also, for $T > 4.2$ K the negative magnetoresistance has vanished, in contrast with the magnetoresistance data of Bayot *et al.* Of course, one cannot exclude that besides the stacking disorder, other structural defects, like vacancies or impurity atoms, contribute to the disorder and hence to the weak localization. It is however beyond the scope of this work to quantify all structural defects.

VI. CONCLUSIONS

The magnetotransport properties of a series of exfoliated graphite foils have been studied at low temperatures ($T > 0.4$ K) and in magnetic fields up to 8 T. All foils show the main features of weak localization: a logarithmic dependence of the resistance on temperature ($T < 2.5$ K) and a negative magnetoresistance in low magnetic fields ($B < 0.5$ T). The negative magnetoresistance can be explained by the theory of quantum corrections to the conductivity for the 2D case. The data were analyzed within the model of Wittmann and Schmid for weak localization beyond the diffusion limit. The analysis of the magnetoresistance yields the phase relaxation

time of the carrier wave. The weak localization is attributed to disorder in the stacking sequence of the graphene layers.

The effect of structural differences in the foils on the negative magnetoresistance was investigated by varying the density and the temperature at which the samples were heat treated. The negative magnetoresistance did not change significantly with the density, indicating that intergrain scattering processes play a minor role. X-ray analysis of the exfoliated graphite samples revealed that the number of turbostratic layers is small, and, therefore, the quantum correction to the conductivity is small. The structural disorder induced by the turbostratic layers is the most likely cause of the weak localization. This is established by annealing the exfoliated graphite foils at $T = 2800$ °C: the negative magnetoresistance becomes significantly smaller, while the disorder in the stacking sequence decreases.

---

*Author to whom correspondence should be addressed. FAX: +31 20 525 5788. Electronic address: schaijk@phys.uva.nl

[1] J. C. Charlier and J. P. Issi, J. Phys. Chem. Solids **57**, 957 (1996).

[2] N. B. Brandt, S. M. Chudinov, and Ya. G. Ponomarev, in *Modern Problems in Condensed Matter Sciences*, edited by V. M. Agranovich and A. A. Maradudin (North-Holland, Amsterdam, 1988), Vol. 20.1.

[3] J. P. Issi, in *Graphite Intercalation Compounds II*, edited by H. Zabel and S. A. Solin (Springer-Verlag, Berlin, 1992), p. 195.

[4] V. A. Kulbachinskii, Phys. Status Solidi B **151**, 185 (1989).

[5] G. M. T. Foley, C. Zeller, E. R. Falardeau, and F. L. Vogel, Solid State Commun. **24**, 371 (1977).

[6] V. A. Kulbachinskii, S. G. Ionov, S. A. Lapin, and A. de Visser, Phys. Rev. B **51**, 10 313 (1995).

[7] V. Bayot, L. Piraux, J. P. Michenaud, J. P. Issi, M. Lelaurain, and A. Moore, Phys. Rev. B **41**, 11 770 (1990).

[8] For a review, see G. Bergmann, Phys. Rep. **107**, 1 (1984); P. A. Lee and T. V. Ramakrishnan, Rev. Mod. Phys. **57**, 287 (1985); S. Chakravarty and A. Schmid, Phys. Rep. **140**, 193 (1986).

[9] H. P. Wittmann and A. Schmid, J. Low Temp. Phys. **69**, 131 (1987).

[10] V. V. Avdeev, L. A. Monyakina, I. V. Nikol'skaya, and S. G. Ionov, Mol. Cryst. Liq. Cryst. Sci. Technol., Sect. A **244**, 115 (1994).

[11] V. A. Kulbachinskii, S. G. Ionov, V. V. Avdeev, N. B. Brandt, S. A. Lapin, A. G. Mandrea, I. V. Kuzmin, and A. de Visser, J. Phys. Chem. Solids **57**, 893 (1996).

[12] W. Ruland, in *Chemistry and Physics of Carbon*, edited by P. L. Walker, Jr. and P. A. Thrower (Dekker, New York, 1968), Vol. 4.

[13] D. E. Soule, Phys. Rev. **112**, 698 (1958).

[14] R. A. Smith, *Semiconductors* (Cambridge University Press, Cambridge, 1978).

[15] B. L. Al'tshuler and A. G. Aranov, in *Modern Problems in Condensed Matter Sciences*, edited by A. L. Efros and M. Pollak (North-Holland, Amsterdam, 1985), Vol. 10.

[16] B. J. F. Lin, M. A. Paalanen, A. C. Gossard, and D. C. Tsui, Phys. Rev. B **29**, 927 (1984).

[17] S. Hikami, A. I. Larkin, and Y. Nagaoka, Prog. Theor. Phys. **63**, 707 (1980).

[18] D. Rainer and G. Bergmann, Phys. Rev. B **32**, 3522 (1985).